ELSEVIER

Chemical Engineering Journal 70 (1998) 197–202

Chemical Engineering Journal

Primary nucleation of citric acid monohydrate: influence of selected impurities

M. Bravi, B. Mazzarotta *

Department of Chemical Engineering, University of Rome 'La Sapienza' Via Eudossiana 18, 00184, Rome, Italy

Received 16 October 1997; received in revised form 2 April 1998; accepted 26 April 1998

Abstract

An experimental study is presented concerning solubility and primary nucleation kinetics of monohydrate citric acid from pure and selectively impure (KH_2PO_4, $MgSO_4 \cdot 7H_2O$ and $FeSO_4 \cdot 7H_2O$) aqueous solutions. The metastable range of pure solutions is wide, ranging from 6 to 14°C, and the order of primary nucleation, equal to 2.51, is quite low. The addition of the tested impurities, which are usual fermentation aids, at concentrations lower than wt. 1%, produces negligible effects on the solubility and slightly enhances the primary nucleation rate. However, the presence of these compounds modifies the crystal habit at birth: in particular, the addition of $MgSO_4 \cdot 7H_2O$ and $FeSO_4 \cdot 7H_2O$ makes these crystals more elongated, but this effect diminishes as the crystals grow.

Keywords: Nucleation; Citric acid monohydrate; Impurities

1. Introduction

Citric acid is a component widely employed in the food and pharmaceutical industry. Its production is based on the fermentation of glucidic substrates by means of moulds or yeasts; the broths are also added with other compounds, such as mineral nutrients, antifoams, etc. Following the fermentation, a number of purification steps are required to recover the product: it finally crystallizes from the refined aqueous solution in form of citric acid monohydrate (CAM) or anhydrous citric acid, depending on whether the temperature level is below or above 36.6°C, respectively. Laguerie et al. [1] reported the solubility and other physical properties of CAM aqueous solutions, Nývlt and Vaclavu [2], Laguerie and Angelino [3], Laguerie et al. [4] investigated the growth kinetics of large CAM crystals and Sikdar and Randolph [5] and Berglund and Larson [6,7] of very small ones; Sikdar and Randolph [5] also studied the secondary nucleation kinetics. Therefore, no data seem to be available concerning the primary nucleation kinetics.

For this reason, an experimental investigation, concerning solubility and primary nucleation kinetics of pure and selectively impure CAM solutions, was performed.

2. Experimental

CAM and the other chemicals used in this work were supplied by Carlo Erba at analytical grade (99.5% wt.).

The experiments were performed in a 200 ml-cell fitted with a jacket through which a temperature controlled liquid was circulated. Mixing was provided by a magnetic stirrer rotating at 850 rpm and the temperature was measured by a probe with 0.02°C accuracy.

2.1. Solubility

First, the solubility temperature of CAM solutions was determined: distilled water and CAM in excess were mixed in the cell and were maintained at constant temperature (±0.1°C) for 48 h. Then, mixing was stopped and the suspension was allowed to settle for 2 h to allow complete sedimentation of the fine crystals: 3 samples, about 2 ml each, were carefully withdrawn from the clear solution using 5 ml pipettes. The samples were titrated with a 1 N solution of NaOH, in the presence of phenolphthalein as indicator. The amounts of CAM solution and titrant were weighed with a scale accurate to 0.0001 g, to ensure a better accuracy than the usual volumetric determinations.

A total of 8 solubility runs (all duplicated) were carried out, at temperatures ranging from 14 to 36°C. The measured concentrations were reproducible within 0.001 kg/kg solu-

---

* Corresponding author. Tel.: +39 06 44585590; Fax: +39 06 4827453; E-mail: barbar@impchim.ing.uniroma1.it

1385-8947/98/$ - see front matter
PII S1385-8947(98)00092-8

tion. However, due to the high viscosity of the CAM solutions (typically higher than 0.02 Pa s [1]), a temperature gradient establishes within the cell when the stirring is stopped to allow the sedimentation of the solid: the temperature difference between locations close to the wall and on the cell axis may be as high as 0.5°C. To ensure reproducibility of the measurements the temperature probe was installed in a fixed position: on the cell axis 40 mm above the bottom.

2.2. Primary nucleation

According to the classical methodology proposed by Nývlt [8], primary nucleation rates can be determined from the metastability range width measurements carried out at different cooling rates. Therefore, solutions prepared from fixed amounts of CAM and distilled water were first heated to a temperature slightly higher than that of solubility, to allow complete dissolution of the solid, then cooled at a fixed constant rate, until nucleation occurred. The latter was easily detected by sight, since very high turbidity suddenly appeared in the solution. Immediately after nucleation occurred, the temperature rapidly increased by 2–3°C, due to the significant heat release associated with the precipitation.

Multiple nucleation temperature determinations were performed for each solution tested, using different cooling rates, varying from $1.67 \cdot 10^{-3}$ to $8.33 \cdot 10^{-3}$ K/s. After nucleation, the suspension was heated at a constant rate of $8.33 \cdot 10^{-3}$ K/s until the residual crystals completely dissolved, and the corresponding dissolution temperature was recorded.

The used thermostatic bath (Pabisch Top Temp 9010) ensured that the desired cooling rate (±10%) was maintained; the measurements of the nucleation and dissolution temperature were reproducible within 0.1°C.

Three series of experiments were carried out for pure solutions at different CAM concentration, ranging from 0.677 to 0.704 kg/kg solution, as listed in Table 1. Then, four series of experimental runs were performed adding to a CAM solution at concentration 0.704 kg/kg solution fixed amounts of KH_2PO_4, $MgSO_4 \cdot 7H_2O$ and $FeSO_4 \cdot 7H_2O$, each at a time, and all together (see Table 1).

Small quantities of these compounds are generally used to improve citric acid fermentation: on the basis of their typical concentrations in the broth [9], those in the CAM solutions were set at the following values: 0.005 kg/kg solution for KH_2PO_4, 0.0005 kg/kg solution for $MgSO4 \cdot 7H_2O$, and 0.001 kg/kg solution for $FeSO_4 \cdot 7H_2O$.

2.3. Crystal habit

In order to investigate the habit of the crystals at birth, samples of suspensions were withdrawn from the cell using pipettes just after nucleation occurred, and immediately observed under an optical Olympus BH-2 microscope, equipped with a camera. Then, 2–3 photographs of each sample were taken as quickly as possible, since the evaporation of the solution under the light of the instrument caused a rapid growth of the nuclei, whose initial size was estimated to be around 5 μm. Small crystals from both pure and selectively impure CAM solutions were submitted to this examination.

3. Results and discussion

3.1. Solubility

The values of CAM equilibrium concentration obtained are shown vs. the temperature in Fig. 1: they exhibit a regular trend, increasing with increasing temperature.

The solubility of pure CAM solutions was previously measured by Laguerie et al. [1] in the range 17–36°C, for a product of purity greater than 99.5% using a technique similar to that adopted in the present work. The results obtained by these authors, also shown in Fig. 1, appear in good agreement with the present one.

The following expression was then used to correlate all the available solubility data as a function of the absolute temperature:

$$\log w_s = 2.094 - \frac{741}{T} \quad (1)$$

Table 1
Operating conditions and results of the experimental runs

Series No.	1	2	3	4	5	6	7
CAM (kg/kg solution)	0.6770	0.7026	0.7036	0.7036	0.7036	0.7036	0.7036
KH_2PO_4 (kg/kg solution)	–	–	–	0.005	–	–	0.005
$MgSO_4 \cdot 7H_2O$ (kg/kg solution)	–	–	–	–	0.0005	–	0.0005
$FeSO_4 \cdot 7H_2O$ (kg/kg solution)	–	–	–	–	–	0.01	0.01
T_{diss} (°C)	26.4	31.1	31.3	30.8	31.5	31.2	30.8
T_s (°C)	25.1	29.8	30.0	29.5	30.2	29.9	29.5
T_n (°C) at $b=0.00167$ K/s	18.3	23.2					
T_n (°C) at $b=0.00333$ K/s	17.8	21.9					
T_n (°C) at $b=0.00416$ K/s			21.3	21.0	21.3	22.0	20.5
T_n (°C) at $b=0.00500$ K/s	15.6	19.5					
T_n (°C) at $b=0.00667$ K/s	14.2	18.3					
T_n (°C) at $b=0.00833$ K/s			17.8	16.0	20.0	15.9	16.1

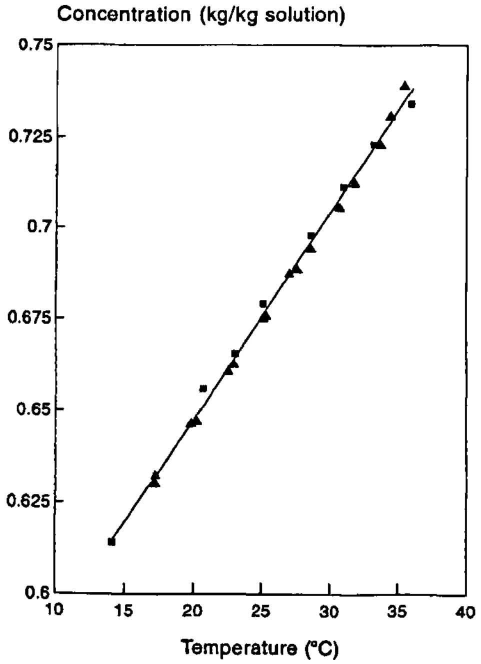

Fig. 1. Solubility of pure CAM solutions vs. temperature: symbols: (■) present experiments; (▲) Ref. [1]; solid line: Eq. (1).

The correlation index is −0.998 and the calculated curve, shown in Fig. 1, appears to accurately describe the solubility of pure CAM solutions.

As far as the impure CAM solutions are concerned, no solubility data are available, and, in the present work, only the dissolution temperatures (listed in Table 1) were measured. According to Mullin [10], such dissolution temperatures can be taken to be the solubility ones when a very low heating rate (2°C/h) is applied. In the present experiments, the heating rate was higher, not allowing the assumption that the dissolution temperature is equal to the solubility temperature, even if the two values appeared strictly linked. In fact, for all the investigated concentrations, the dissolution temperatures recorded for pure CAM solutions was found to be 1.3°C higher than the corresponding solubility temperatures. By assuming that the difference between the solubility and the dissolution temperatures depended only on the adopted heating rate and was not related to the composition of the solution, the solubility temperatures of the impure solutions were then estimated by subtracting 1.3°C from the measured dissolution temperatures: their values are listed in Table 1.

It can be noted that the solubility temperatures of the impure CAM solutions do not differ too much from those of the pure ones: in the presence of the impurities the solubility temperature generally decreases of 0.1–0.5°C, with the exception of $MgSO_4 \cdot 7H_2O$, whose addition causes a slight increase (0.2°C) of the solubility temperature. Although the magnitude of the observed deviations is very small, they were well reproducible, indicating a real, even if small effect of the tested compounds on the solubility. The influence of the selected impurities is not proportional to their concentration: in fact, the lowest effect is observed for $FeSO_4 \cdot 7H_2O$, whose concentration was the highest one. In general, the influence of the sulphates appears more limited than that of the phosphate, and the effect of the latter prevails also when all the compounds are simultaneously present.

3.2. Primary nucleation

The primary nucleation rate, R_n, is usually expressed as a function of the supersaturation Δw:

$$R_n = k_n \Delta w^m \tag{2}$$

with k_n nucleation constant and m order of nucleation.

According to Nývlt [8], the nucleation rate can also be expressed as:

$$R_n = b \left.\frac{\mathrm{d}w}{\mathrm{d}T}\right|_{T=T_n} \tag{3}$$

where b is the cooling rate and the derivative term represents the slope of the solubility curve calculated at the nucleation temperature.

By combining Eqs. (2) and (3), the values of the nucleation order and constant can be calculated by a log–log correlation of metastability zone width measurements at different cooling rates.

The nucleation temperatures determined in the experiments are listed in Table 1: the metastable zone width ranges from 6 to 14°C, being larger when the cooling rate is higher, as expected [10].

The addition of the selected impurities does not change significantly these values, although it generally causes a slight increase of the metastable zone width, more significant (up to 2°C) in the case of addition of $FeSO_4 \cdot 7H_2O$; on the contrary, the addition of $MgSO_4 \cdot 7H_2O$ appears to exhibit an opposite effect. This behaviour was expected, based on the influence of the examined compounds on the solubility: in fact, as reported by Nývlt [8], a higher solubility should give rise to a lower metastability range width.

Eq. (1) was used to calculate CAM concentration at the nucleation temperature; the slope of the solubility curve, which appears in Eq. (3), was estimated analytically as the derivative of Eq. (1), whose value was calculated at a temperature corresponding to the average value obtained from the nucleation experiments.

The metastable zone width data relevant to pure CAM (experiments belonging to series 1–3), expressed in concentration terms, appeared well aligned vs. the cooling rate, on a log–log plot (see Fig. 2): the data were fitted using the least squares method and the values of nucleation order and constant listed in Table 2 were calculated.

For the impure CAM solutions, the simplifying assumption was made that the solubility curve obtained for pure CAM simply moved toward higher or lower values, depending on the observed deviations of the solubility temperature, without changing its shape. Accordingly, the equilibrium concentrations were still calculated using Eq. (1), just applying the

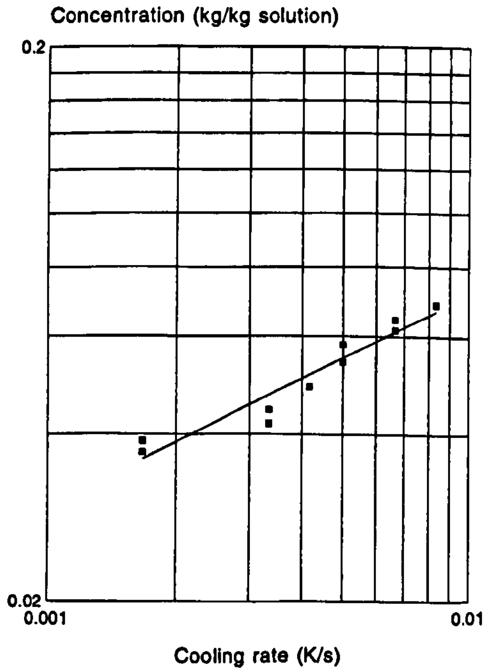

Fig. 2. Metastable zone width in concentration terms vs. cooling rate for pure CAM solutions.

following correction, derived from Table 1, to the temperature values: addition of $KH_2PO_4 = -0.5°C$; addition of $FeSO_4 \cdot 7H_2O = -0.1°C$; addition of $MgSO_4 \cdot 7H_2O = +0.2°C$; simultaneous addition of all the 3 impurities $= -0.5°C$.

The nucleation parameters were then determined as described above: their values are listed in Table 2. It can be noticed that, for the impure solutions, the nucleation order varies from 1.1 to 4.7, being lower than that of pure CAM (2.51) in case of addition of KH_2PO_4, $FeSO_4 \cdot 7H_2O$ and of the 3 impurities at the same time, and higher only in the case of addition of $MgSO_4 \cdot 7H_2O$, which exhibits its own peculiar influence, as previously observed.

Fig. 3 compares the primary nucleation kinetics for pure and impure CAM solutions. The effect of the presence of the impurities can be clearly detected, but the nucleation rates do not change substantially; generally, in case of impure solutions, the kinetics slightly increase, especially at low supersaturation. The addition of $MgSO_4 \cdot 7H_2O$ causes an opposite effect, i.e., a decrease of the kinetics at low supersaturation and an increase at high supersaturation.

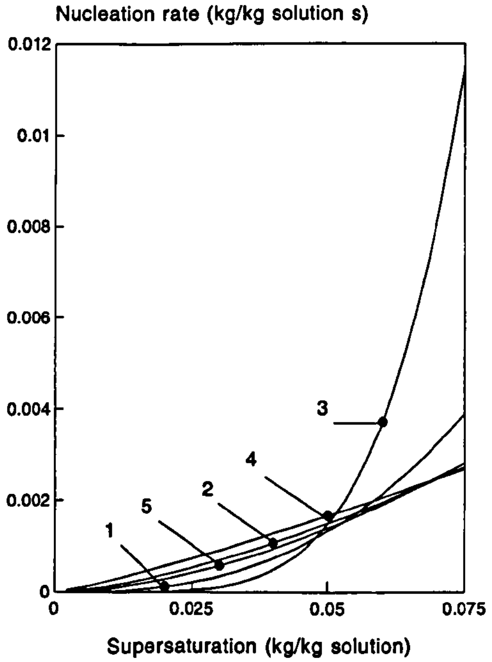

Fig. 3. Comparison of the nucleation rates of pure and selectively impure CAM solutions: (1) Pure CAM solution; (2) KH_2PO_4 impure solution; (3) $MgSO_4 \cdot 7H_2O$ impure solution; (4) $FeSO_4 \cdot 7H_2O$ impure solution; (5) KH_2PO_4 $MgSO_4 \cdot 7H_2O$ and $FeSO_4 \cdot 7H_2O$ impure solution.

3.3. Crystal habit

Pure CAM crystals exhibit an orthorhombic structure, which is that usual for this compound: the lengths of the three axes are comparable (Fig. 4a). The addition of the tested impurities appears capable of modifying the crystal habit. In particular, the addition of KH_2PO_4 causes the crystals structure to move toward a dipyramidal shape, but without appreciable alteration of the axes ratios (Fig. 4b). The addition of the sulphates results in a more pronounced effect, since the shape becomes elongated (Fig. 4c,d), particularly in the presence of $FeSO_4 \cdot 7H_2O$ (see Fig. 4c, where the main axis of the nuclei appears almost double in length compared to that of the pure product). When all the tested impurities are added simultaneously the various habit modifications appear to coexist (Fig. 4e). However, the simultaneous presence of both sulphates did not exhalt the elongating effect: this is

Table 2
Values of the nucleation parameters

Characteristics of the aqueous solution	k^n	m
Pure CAM solution	3.62	2.64
CAM solution added with 0.005 $kg/kg_{solution} KH_2PO_4$	0.130	1.49
CAM solution added with 0.0005 $kg/kg_{solution} MgSO_4 \cdot 7H_2O$	5664	5.06
CAM solution added with 0.01 $kg/kg_{solution}$ of $FeSO_4 \cdot 7H_2O$	0.0572	1.18
CAM solution added with 0.005 $kg/kg_{solution}$ KH_2PO_4, 0.0005 $kg/kg_{solution}$ $MgSO_4 \cdot 7H_2O$ and 0.01 $kg/kg_{solution}$ $FeSO_4 \cdot 7H_2O$	0.256	1.74

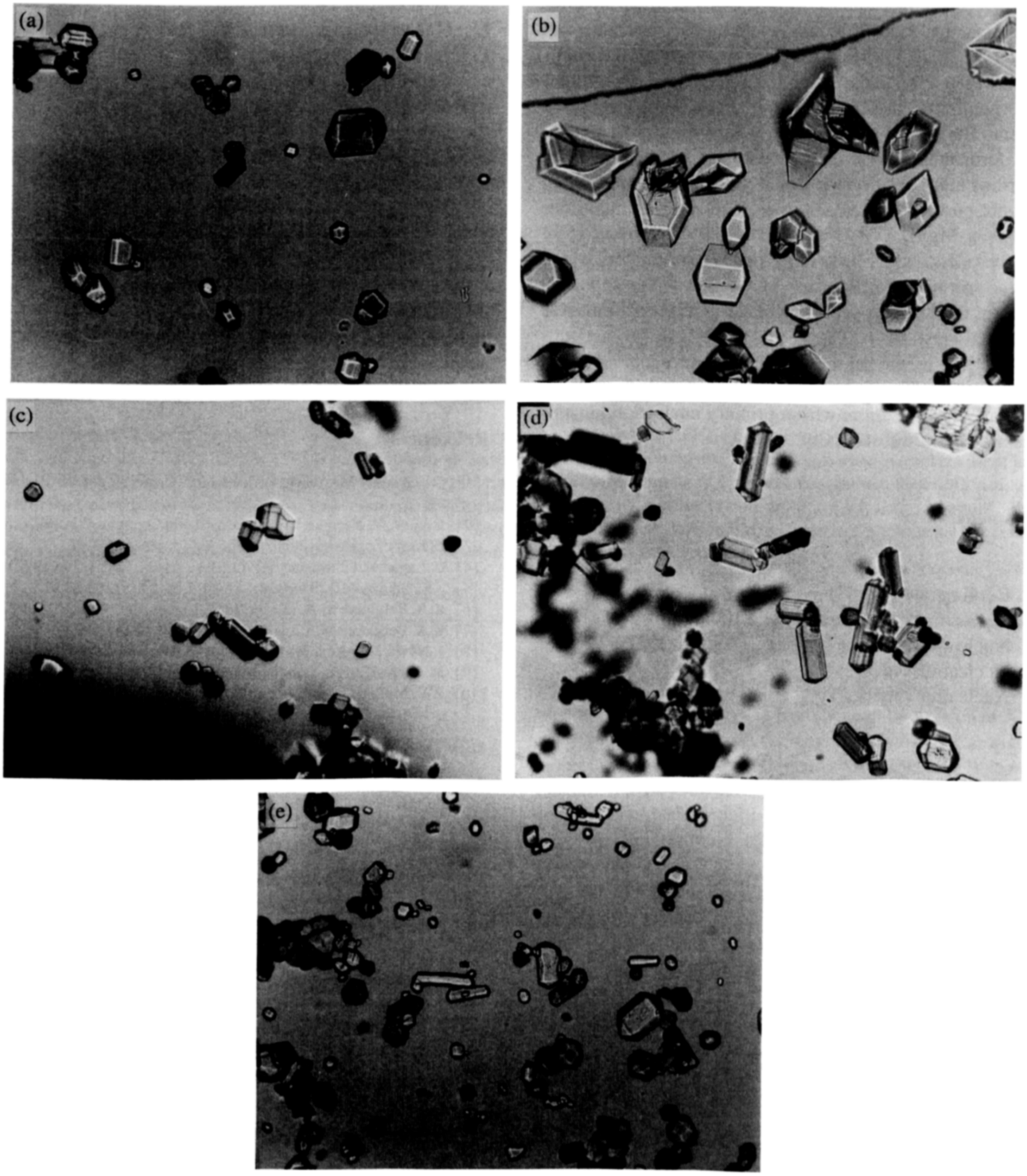

Fig. 4. Crystal habit: (a) Pure CAM crystals; (b) KH_2PO_4 impure solution; (c) $MgSO_4 \cdot 7H_2O$ impure solution; (d) $FeSO_4 \cdot 7H_2O$ impure solution; (e) KH_2PO_4 $MgSO_4 \cdot 7H_2O$ and $FeSO_4 \cdot 7H_2O$ impure solution.

important, since the addition of these compounds may potentially give rise to needle-like crystals, which are liable to be more fragile.

All the photographs were taken under the same magnification and using almost identical procedures: the length of the smallest particles is about 5 μm, the largest being more than 50 μm in size. It has to be remarked that the differences in the crystal habit induced by the presence of the impurities become less significant as the crystals grow over 100 μm.

4. Conclusions

In this work the primary nucleation kinetics of CAM were determined according with the classical method of Nývlt [8]:

the range of the metastable zone width was quite large, in terms of temperature difference, and the nucleation order was not very high. These results, which have favourable implication with respect to the crystallization process, are substantially confirmed also when some selected impurities are present. The latter were chosen among the more frequently used fermentation aids and their concentration was fixed according to the expected residual content in the concentrated (but not purified) CAM solutions. The selected impurities (KH_2PO_4, $MgSO_4 \cdot 7H_2O$ and $FeSO_4 \cdot 7H_2O$) showed some influence also over the habit of the newly born crystals, which became more elongated in case of addition of the sulphates; however, this effect appears to lose most of its importance as the crystal grew.

According to the present results, the presence of small traces of these fermentation aids produce a moderate effect on CAM crystallization, whose primary nucleation kinetics does not change substantially.

5. Nomenclature

b	Cooling rate ($K\ s^{-1}$)
c_s	Equilibrium concentration ($kg\ 100\ g^{-1}$ water)
k_n	Nucleation constant ($(kg\ kg^{-1}\ solution)^{1-m}\ s^{-1}$)
m	Nucleation order
R_n	Nucleation rate ($kg\ kg^{-1}\ solution\ s^{-1}$)
T	Temperature (K)
T_n	Nucleation temperature (°C)
T_s	Solubility temperature (°C)
w	Concentration ($kg\ kg^{-1}$ solution)
w^*	Equilibrium concentration ($kg\ kg^{-1}$ solution)
Δw	supersaturation ($kg\ kg^{-1}$ solution)

Acknowledgements

This work was financially supported by the Italian Research Council. The collaboration of Mr. M. Castellano and Ms. S. Antonioli for the experimental work is gratefully acknowledged.

References

[1] C. Laguerie, M. Aubry, J. Couderc, J. Chem. Eng. Data 21 (1976) 85.
[2] J. Nývlt, V. Vaclavu, Coll. Czech. Chem. Commun. 37 (1972) 3664.
[3] C. Laguerie, H. Angelino, Chem. Eng. J. 10 (1975) 41.
[4] C. Laguerie, G. Muratet, H. Angelino, Chem. Eng. J. 14 (1977) 17.
[5] S.K. Sikdar, A.D. Randolph, AIChE J. 22 (1) (1976) 110.
[6] K.A. Berglund, M.A. Larson, AIChE Symp. Ser. 78 (215) (1982) 9.
[7] K.A. Berglund, M.A. Larson, AIChE J. 30 (1984) 280.
[8] J. Nývlt, J. Cryst. Growth 3–4 (1968) 377.
[9] M. Moresi, private communication.
[10] J.W. Mullin, Crystallisation, 2nd edn., Butterworth, London, 1972.